doi:10.1038/nature10980

Hsp72 preserves muscle function and slows progression of severe muscular dystrophy

Stefan M. Gehrig[1], Chris van der Poel[1]†, Timothy A. Sayer[1], Jonathan D. Schertzer[1]†, Darren C. Henstridge[2], Jarrod E. Church[1]†, Severine Lamon[3], Aaron P. Russell[3], Kay E. Davies[4], Mark A. Febbraio[2] & Gordon S. Lynch[1]

Duchenne muscular dystrophy (DMD) is a severe and progressive muscle wasting disorder caused by mutations in the dystrophin gene that result in the absence of the membrane-stabilizing protein dystrophin[1–3]. Dystrophin-deficient muscle fibres are fragile and susceptible to an influx of Ca^{2+}, which activates inflammatory and muscle degenerative pathways[4–6]. At present there is no cure for DMD, and existing therapies are ineffective. Here we show that increasing the expression of intramuscular heat shock protein 72 (Hsp72) preserves muscle strength and ameliorates the dystrophic pathology in two mouse models of muscular dystrophy. Treatment with BGP-15 (a pharmacological inducer of Hsp72 currently in clinical trials for diabetes) improved muscle architecture, strength and contractile function in severely affected diaphragm muscles in *mdx* dystrophic mice. In *dko* mice, a phenocopy of DMD that results in severe spinal curvature (kyphosis), muscle weakness and premature death[7,8], BGP-15 decreased kyphosis, improved the dystrophic pathophysiology in limb and diaphragm muscles and extended lifespan. We found that the sarcoplasmic/endoplasmic reticulum Ca^{2+}-ATPase (SERCA, the main protein responsible for the removal of intracellular Ca^{2+}) is dysfunctional in severely affected muscles of *mdx* and *dko* mice, and that Hsp72 interacts with SERCA to preserve its function under conditions of stress, ultimately contributing to the decreased muscle degeneration seen with Hsp72 upregulation. Treatment with BGP-15 similarly increased SERCA activity in dystrophic skeletal muscles. Our results provide evidence that increasing the expression of Hsp72 in muscle (through the administration of BGP-15) has significant therapeutic potential for DMD and related conditions, either as a self-contained therapy or as an adjuvant with other potential treatments, including gene, cell and pharmacological therapies.

DMD is the most severe form of muscular dystrophy; it affects about 1 in 3,500 live male births[1]. Intracellular Ca^{2+} regulation is compromised in dystrophic muscle fibres, which triggers chronic inflammation, repeated cycles of degeneration with progressively ineffective regeneration, and infiltration of fibrotic and other non-contractile material[4]. Mechanisms for the influx of Ca^{2+} into dystrophic muscle fibres include membrane tears[4–6], stretch-activated channels[9], Ca^{2+} leak channels[10] and leaky Ca^{2+} release channels[11], and it has been speculated that the function of SERCA, the main protein responsible for Ca^{2+} reuptake into the sarcoplasmic reticulum (SR), is compromised[12,13]. Increasing SERCA pump expression within dystrophic muscles in transgenic mice or through viral-mediated delivery improves Ca^{2+} handling and suppresses the pathological cascade of events[14,15]. The role of inflammation in the dystrophic pathology is well known, particularly that of the pro-inflammatory cytokine tumour necrosis factor-α (TNF-α)[16]. TNF-α activates the nuclear factor-κB (NF-κB) and c-Jun N-terminal kinase (JNK) signalling pathways[17–19]. Hsp72 is a molecular chaperone protein that inhibits inflammatory mediators including p-JNK, TNF-α and the NF-κB pathway[20–22], and binds and preserves SERCA function under conditions of cellular stress[23]. Although some studies have shown Hsp72 to be elevated in patients with DMD[24], there is little consensus, because expression data for young patients are variable and sourcing age-matched controls is problematic (Supplementary Fig. 1a). Nevertheless, the endogenous heat shock protein response in DMD is insufficient to be protective. Here we tested the hypothesis that increasing the levels of Hsp72 protects dystrophic muscles from functional deterioration. We bred dystrophin-null *mdx* dystrophic mice with mice showing a muscle-specific transgenic (TG) overexpression of Hsp72, producing $mdx^{TG(+)}$ mice and *mdx* littermate controls (Fig. 1a; see Supplementary Fig. 1b for quantification). At about 25 weeks of age, serum levels of creatine kinase (CK), a classic indicator of muscle breakdown, were decreased in $mdx^{TG(+)}$ mice compared with littermate control mice lacking the transgene ($mdx^{TG(-)}$; Fig. 1b). Because most patients with DMD show severe weakness[4] and/or muscle fatigue[25], we assessed whole-body strength and endurance in dystrophic mice by using a hang test to measure latency-to-fall, which was significantly improved in $mdx^{TG(+)}$ mice (24 ± 3 s versus 64 ± 14 s; $P = 0.002$, $n \geq 20$ mice). Respiratory failure is the cause of death in up to 90% of patients with DMD[26], and because diaphragm function is an accurate predictor of respiratory insufficiency we investigated the effect of Hsp72 overexpression on the pathophysiology of the diaphragm in dystrophin-deficient mice. The progressive degeneration of the diaphragm in *mdx* mice closely mimics that in DMD[27]. Gross histological analyses revealed that the diaphragm pathology in $mdx^{TG(+)}$ mice was ameliorated compared with age-matched littermate control $mdx^{TG(-)}$ mice (Supplementary Fig. 1c), an observation supported by the minimal Feret's diameter variance coefficient, which provides a sensitive measure of fibre heterogeneity and the dystrophic pathology[28]. We found a lower Feret's diameter variance coefficient in $mdx^{TG(+)}$ mice than in $mdx^{TG(-)}$ mice, indicative of an improved phenotype (405 ± 5 versus 358 ± 5; $P < 0.001$, $n = 5$). Damaged myofibres can be revealed by the infiltration of Evans blue dye (EBD) entering the myoplasm through tears in the sarcolemma[4–6]. EBD infiltration was decreased in cross-sections of the diaphragm from $mdx^{TG(+)}$ mice in comparison with that from $mdx^{TG(-)}$ mice (Fig. 1c and Supplementary Fig. 1d), indicative of decreased necrosis and hastened overall repair of damaged fibres rather than improved structural integrity. To support this contention, we performed well-described *in situ* and *in vitro* contraction-induced injury protocols on tibialis anterior (TA) and diaphragm muscles, respectively (see Methods). No differences in contraction-mediated damage were evident between muscles of $mdx^{TG(+)}$ and $mdx^{TG(-)}$ mice (Supplementary Fig. 1e), indicating that structural integrity was unaltered. Expression of the dystrophin homologue, utrophin, a protein known to compensate for the loss of dystrophin, was also unchanged (Supplementary Fig. 1f). We assessed collagen infiltration in sections of

[1]Basic and Clinical Myology Laboratory, Department of Physiology, University of Melbourne, Victoria, 3010, Australia. [2]Cellular and Molecular Metabolism Laboratory, Baker-IDI Heart and Diabetes Institute, PO Box 6492, St Kilda Road Central, Victoria, 8008, Australia. [3]Centre for Physical Activity and Nutrition Research, School of Exercise and Nutrition Sciences, Deakin University, Burwood, Victoria, 3125, Australia. [4]MRC Functional Genomics Unit, Department of Physiology, Anatomy and Genetics, University of Oxford, South Parks Road, Oxford OX1 3QX, UK. †Present addresses: Department of Human Biosciences, Faculty of Health Sciences, La Trobe University, Bundoora, 3086, Victoria, Australia (C.v.d.P. and J.E.C.); Department of Biochemistry and Biomedical Sciences and Department of Pediatrics, McMaster University, Hamilton, Ontario, L8S 4L8, Canada (J.D.S.).

©2012 Macmillan Publishers Limited. All rights reserved

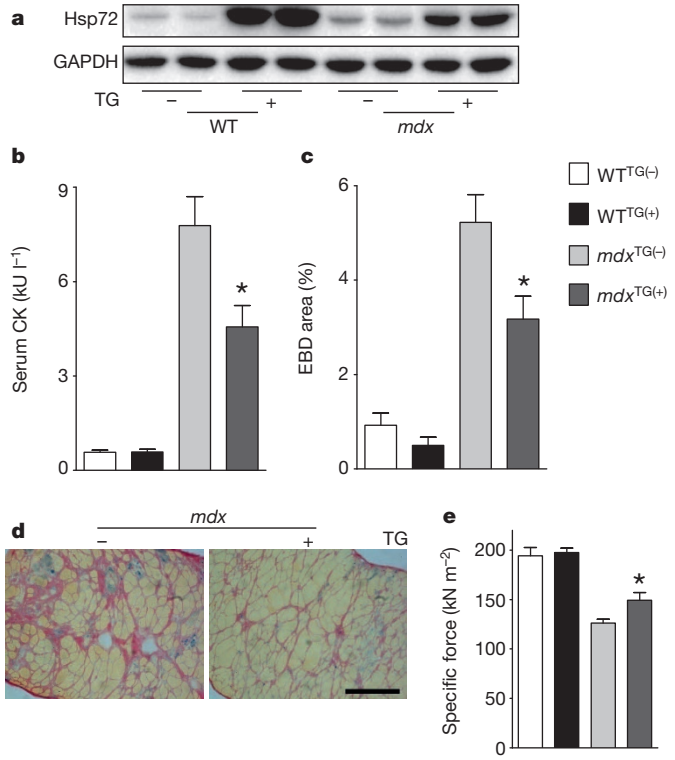

Figure 1 | Transgenic Hsp72 overexpression increases muscle strength, decreases muscle breakdown and improves diaphragm muscle histological parameters in *mdx* mice. **a**, Representative western blot detection of Hsp72 in diaphragm muscle homogenates from non-dystrophic (WT) and dystrophic (*mdx*) Hsp72 transgene-negative (TG−) and transgene-positive (TG+) mice. GAPDH, glyceraldehyde-3-phosphate dehydrogenase. **b**, Whole-body muscle breakdown, measured by serum creatine kinase (CK) levels. Asterisk, $P < 0.05$, $n \geq 6$. **c**, Quantified mean data for EBD-positive area in diaphragm muscle sections. Asterisk, $P < 0.05$, $n \geq 4$. **d**, Representative images of collagen infiltration in diaphragm sections (revealed with Van Gieson's stain) from $mdx^{TG(-)}$ and $mdx^{TG(+)}$ mice. **e**, Specific (normalized) force of diaphragm muscle strips measured *in vitro*. Asterisk, $P < 0.05$, $n \geq 5$. All data are from 25-week-old mice. Scale bar, 200 μm. Data are shown as means ± s.e.m.

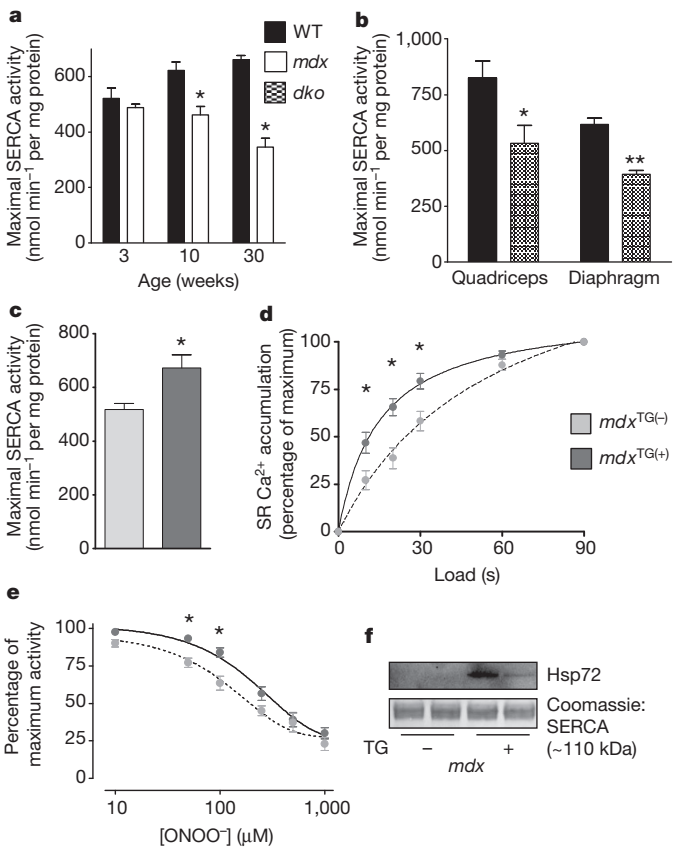

Figure 2 | Maximal SERCA activity is decreased in mouse models of dystrophy; Hsp72 binding improves SERCA function. **a**, Maximal SERCA activity in diaphragm muscle homogenates from WT and *mdx* mice at 3, 10 and 30 weeks of age. Asterisk, $P < 0.001$, $n \geq 4$. **b**, Maximal SERCA activity of muscle homogenates from quadriceps and diaphragm from 10-week-old WT and *dko* mice. Asterisk, $P = 0.036$. Two asterisks, $P < 0.001$, $n \geq 4$. **c**, Maximal SERCA activity in muscle homogenates from $mdx^{TG(-)}$ (pale grey bars) and $mdx^{TG(+)}$ (dark grey bars) mice. Asterisk, $P < 0.008$, $n \geq 9$. **d**, Ca^{2+} accumulation curves (an indirect measure of SERCA activity) for SR in single fibres from extensor digitorum longus muscles of $mdx^{TG(-)}$ and $mdx^{TG(+)}$ mice. Asterisk, $P < 0.01$, $n \geq 15$. **e**, Maximal SERCA activity after incubation for 5 min at various concentrations of peroxynitrite ($ONOO^-$), measured in enriched SR vesicles isolated from muscles of $mdx^{TG(-)}$ and $mdx^{TG(+)}$. SERCA activity was normalized to maximal activity in the absence of $ONOO^-$. Asterisk, $P < 0.05$, $n \geq 3$. **f**, Representative western blots of enriched SR vesicles from $mdx^{TG(-)}$ and $mdx^{TG(+)}$ ($n = 4$) mice, showing Hsp72 protein expression and Coomassie blue stain (showing SERCA isoforms). Data are shown as means ± s.e.m.

diaphragm and found that $mdx^{TG(+)}$ mice had less collagen infiltration than $mdx^{TG(-)}$ mice at both 25 weeks of age (Fig. 1d and Supplementary Fig. 1g) and 80 weeks of age (data not shown). Normalized force production was significantly higher in diaphragm muscle strips from $mdx^{TG(+)}$ mice than in those from $mdx^{TG(-)}$ mice (Fig. 1e).

We have shown that Hsp72 can block inflammation in mice *in vivo*[22], and because inflammation promotes muscle degeneration in mouse models of DMD[17] we examined the effect of Hsp72 on expression of p-JNK, p-IKK (a key mediator of NF-κB activation) and TNF-α. Western blot and polymerase chain reaction (PCR) analyses revealed no difference in these inflammatory markers in diaphragm muscles from $mdx^{TG(-)}$ and $mdx^{TG(+)}$ mice (Supplementary Fig. 2, and data not shown). There was significantly decreased messenger RNA expression of macrophage markers CD68 and F4/80 and TNF-α in TA muscles of $mdx^{TG(+)}$ mice (Supplementary Fig. 3), but these did not translate to functional improvements (data not shown). We next examined SERCA activity in diaphragm muscles from wild-type (WT) and *mdx* mice and showed a progressive age-related decline in maximal SERCA activity in *mdx* mice (Fig. 2a and Supplementary Fig. 4a), despite an age-related increase in SERCA protein expression (Supplementary Fig. 4b). This functional decline is attributed, in part, to post-translational modifications of the SERCA protein, especially nitrosylation, which decreases maximal SERCA activity as a result of changes in Ca^{2+}-binding and ATP-binding domains[23]. Alterations in the Ca^{2+}-binding domain changes SERCA enzyme kinetics, decreasing Ca^{2+} sensitivity and increasing $[Ca^{2+}]_{50}$ (the $[Ca^{2+}]$ required to achieve half-maximal enzyme activity), an effect we observed in diaphragm muscles from 30-week-old *mdx* mice (Supplementary Fig. 4c). Similar deficits in SERCA activity were evident in both limb and diaphragm muscles of severely affected *dko* mice (Fig. 2b), indicating that abnormal SERCA function may contribute to the disruptions in Ca^{2+} regulation characteristic of dystrophic muscles. Indeed, recent evidence suggests that closer regulation of Ca^{2+} homeostasis through enhanced SERCA expression or activity significantly suppresses the degeneration of dystrophic muscle[14,15]. Because Hsp72 binds SERCA and prevents functional inactivation under conditions of cellular stress[23], we next tested the hypothesis that overexpression of Hsp72 in dystrophic muscles would improve SERCA function. We examined maximal SERCA activity in homogenates of quadriceps muscles, and found an increase in activity in $mdx^{TG(+)}$ compared with $mdx^{TG(-)}$ mice (Fig. 2c). To support this finding we also examined Ca^{2+} accumulation in SR (an indirect measure of SERCA activity) in single muscle fibres dissected from fast-twitch

©2012 Macmillan Publishers Limited. All rights reserved

extensor digitorum longus, and predominantly slow-twitch soleus muscles, and found a similar increase in maximal SERCA activity in individual muscle fibres in $mdx^{TG(+)}$ compared with $mdx^{TG(-)}$ mice (as for whole-muscle homogenates), with no changes in mRNA for SERCA or in protein expression (Fig. 2d, Supplementary Fig. 5 and Supplementary Table 1). We then examined whether Hsp72 overexpression could protect SERCA function under conditions of stress, like that induced by reactive oxygen–nitrogen species such as peroxynitrite ($ONOO^-$). We developed a SERCA activity assay in which enriched SR vesicles isolated from $mdx^{TG(-)}$ and $mdx^{TG(+)}$ mice were incubated with increasing concentrations of $ONOO^-$; the subsequent suppression in activity was normalized to that in the absence of $ONOO^-$. We found that SERCA activity was greater in the presence of various $ONOO^-$ concentrations in enriched SR vesicles from $mdx^{TG(+)}$ compared with $mdx^{TG(-)}$ mice (Fig. 2e), with western blots revealing Hsp72 protein levels were highly elevated in enriched SR vesicles from $mdx^{TG(+)}$ mice (Fig. 2f; see Supplementary Fig. 6 for full blots), indicating that Hsp72 was bound within the SR to mediate this protective effect. These data indicate that Hsp72 overexpression in dystrophic muscles can protect SERCA from inactivating modifications and is a likely mechanism of protection in $mdx^{TG(+)}$ mice.

Given the significant phenotypic improvements in $mdx^{TG(+)}$ mice, especially in the diaphragm, we examined whether similar effects could be achieved through the pharmacological or heat-therapy induction of Hsp72. BGP-15 is a pharmacological inducer of Hsp72 that can protect against obesity-induced insulin resistance[22] and is in Food and Drug Administration (FDA)-approved Phase II clinical trials for diabetes[29]. Dystrophic *mdx* mice were treated from 4 to 9 weeks of age (5 weeks) or from 4 to 16 weeks of age (12 weeks) with BGP-15 (15 mg kg^{-1} per day, oral gavage). WT mice were used for comparisons with *mdx* mice. Hsp72 protein expression was elevated in diaphragm muscle homogenates from BGP-15-treated *mdx* mice (and heat-therapy-treated mice) compared with untreated *mdx* mice (Fig. 3a; see Supplementary Fig. 7a for quantification). CK levels were decreased in BGP-15-treated *mdx* mice compared with untreated *mdx* mice (Fig. 3b). EBD infiltration was also reduced with long-term BGP-15 treatment (Fig. 3c). Strength and endurance was evaluated with the inverted hang test; WT mice were stronger than *mdx* mice, and BGP-15-treated *mdx* mice showed an increased latency-to-fall compared with control (Supplementary Fig. 7). An increase in fibrosis, as seen in DMD[4], was observed in the *mdx* diaphragm (compared with WT), and BGP-15 treatment significantly decreased fibrosis (Fig. 3d; see Supplementary Fig. 7 for quantification). Treatment with BGP-15 attenuated the functional deterioration of the diaphragm muscle significantly (Fig. 3e). Maximal SERCA activity in diaphragm homogenates was increased in *mdx* mice after long-term treatment with BGP-15, indicating a mechanism consistent with that of transgenic Hsp72 overexpression (Fig. 3f). Because elevated core temperature is a potent inducer of heat shock proteins[22,30], we also extensively tested this method of heat shock protein induction (see Methods). Similar beneficial effects to those observed with transgenic Hsp72 overexpression and BGP-15 treatment were seen in *mdx* mice exposed to repeated heat therapy (see Supplementary Fig. 8).

We then investigated whether treatment with BGP-15 was protective in severely affected dystrophic *dko* mice, the most phenotypically accurate murine model of DMD[7,8] (see Methods). The *dko* mice were treated with BGP-15 from 3–4 weeks until 10 weeks of age. For the survival study, *dko* mice were treated from 3–4 weeks until death or humane killing (as described in Methods). Photographs of control and BGP-15-treated *dko* mice were taken at 10 weeks, immediately before killing, and after evisceration and staining of the skeleton with alizarin red (Fig. 4a). Data from WT mice (as in Fig. 3) were also used for comparisons with *dko* mice. Because boys with DMD have significant paraspinal muscle weakness and in many cases severe kyphosis (spinal curvature)[4,8], this was quantified in conscious mice (from the 10-week endpoint cohort) by a blinded investigator using a 1–5 index of

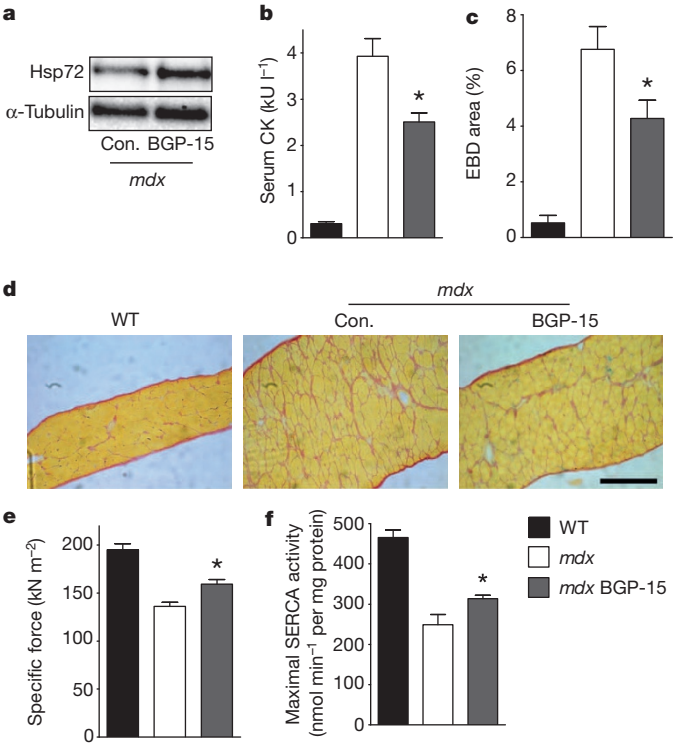

Figure 3 | Pharmacological induction of Hsp72 ameliorates muscular dystrophy in *mdx* mice. **a**, Representative western blot detection of Hsp72 in diaphragm muscle homogenates of control (Con.) and BGP-15-treated *mdx* mice. **b**, Whole-body muscle breakdown, measured by serum CK levels in WT (C57BL/10), *mdx* (control) and BGP-15-treated *mdx* mice. Asterisk, $P < 0.01$, $n \geq 8$. **c**, Quantified mean data for EBD infiltration in *mdx* mice treated for 12 weeks. Asterisk, $P < 0.05$, $n \geq 8$. **d**, Representative images of collagen infiltration in diaphragm muscle sections. **e**, Specific force production in diaphragm muscle strips measured *in vitro*. Asterisk, $P < 0.01$, $n \geq 9$. **f**, Maximal SERCA activity in diaphragm muscle homogenates from *mdx* mice treated for 12 weeks. Asterisk, $P < 0.05$, $n \geq 6$. Scale bar, 200 μm. WT data are used as a reference control. All treated mice received BGP-15 for 5 weeks unless stated otherwise. Data are shown as means ± s.e.m.

kyphosis, 1 indicating no spinal deformity on palpation and 5 being the most severe. Treatment with BGP-15 decreased kyphosis markedly compared with vehicle-treated controls (Fig. 4b). Serum CK levels were significantly lower in *dko* mice after treatment with BGP-15 (Fig. 4c), indicating decreased whole-body muscle breakdown. Collagen infiltration was decreased in the diaphragm of *dko* mice after treatment with BGP-15 (Fig. 4d) and the force-producing capacity of diaphragm muscle strips and intact TA muscles (measured *in situ*) was increased significantly in BGP-15-treated *dko* mice, with maximum force restored to WT levels in the TA muscle (Fig. 4e, f and Supplementary Table 2). No differences in body mass or in calcification or central nucleation within diaphragm muscles were evident in *dko* mice after treatment with BGP-15 (data not shown). However, the most important outcome was that lifelong treatment of *dko* mice with BGP-15 significantly extended survival (Fig. 4g, h; $P < 0.05$; 27% increase in median lifespan). This finding has clinical relevance for DMD.

Our findings reveal that transgenic Hsp72 overexpression improves several pathological indices in *mdx* dystrophic mice, at least in part by preserving or improving SERCA function. Furthermore, treatment of dystrophic mice with BGP-15, a known pharmacological co-inducer of Hsp72, ameliorated the dystrophic pathology and extended the lifespan in *dko* mice. Taken together, these results indicate that induction of Hsp72 in muscular dystrophy is an important and novel therapeutic approach that can improve the dystrophic pathology and attenuate the disease progression. Although an ultimate cure for DMD is likely to be derived from gene or cell therapies, considerable

©2012 Macmillan Publishers Limited. All rights reserved

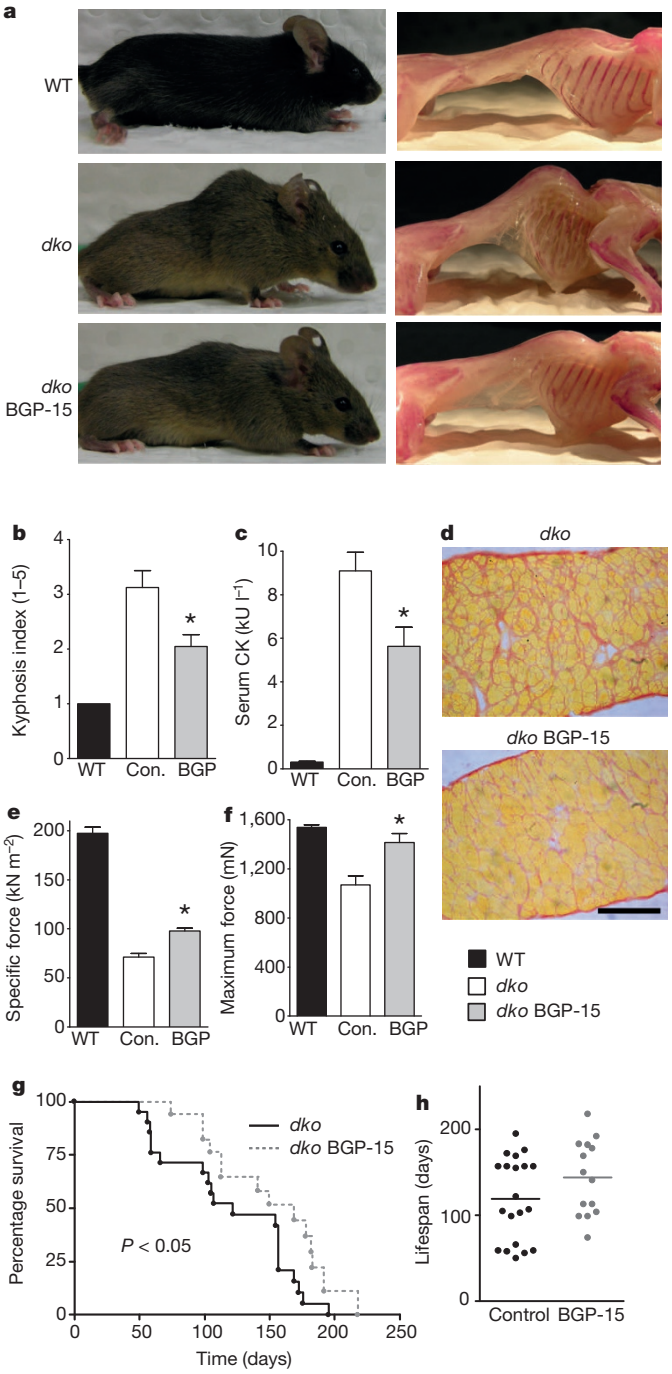

Figure 4 | Treatment with BGP-15 decreases kyphosis (spinal curvature), improves muscle function and prolongs lifespan in severely dystrophic *dko* mice. **a**, Left: representative photographs of WT (C57BL/10), *dko* and BGP-15-treated *dko* mice. Right: representative eviscerated skeletal preparations showing bone structure (pink), and highlighting spinal curvature in *dko* mice. **b**, Spinal curvature was quantified (1–5) in WT, *dko* and BGP-15-treated *dko* mice. Asterisk, $P < 0.05$, $n \geq 10$. **c**, Whole-body muscle breakdown, measured by serum CK levels. Asterisk, $P < 0.05$, $n \geq 8$. **d**, Representative images of collagen infiltration in diaphragm sections. **e**, Specific force of diaphragm muscle strips measured *in vitro*. Asterisk, $P < 0.01$, $n \geq 9$. **f**, Maximal force production in TA measured *in situ*. Asterisk, $P < 0.01$, $n \geq 9$. **g**, Survival curve of untreated (control) and BGP-15-treated *dko* mice. $P < 0.05$, $n \geq 14$. **h**, Scatter-plot of *dko* lifespan with a line showing median survival. Scale bar, 200 μm. WT data are used as a reference control. Data are shown as means ± s.e.m.

obstacles need to be overcome before these approaches can be considered safe and effective. Until these concerns are obviated, alternative (and potentially synergistic) therapies, such as pharmacological induction of Hsp72, could delay the disease progression to allow many patients to benefit from perfected treatments.

In a recent clinical trial for patients with insulin resistance, treatment with BGP-15 (200 mg and 400 mg once a day for 28 days) significantly increased sensitivity to insulin. The dose schedule of BGP-15 was well tolerated, with both doses being safe: there were no clinically significant changes in physical status or in laboratory or electrocardiogram parameters[29]. Given that BGP-15 is currently used in clinical trials for other pathologies, our findings identify it as a tangible and realistic treatment method for patients with DMD in the near future.

METHODS SUMMARY

Animals. All experiments were approved by the Animal Ethics Committee of The University of Melbourne and conducted in accordance with the Australian code of practice for the care and use of animals for scientific purposes as stipulated by the National Health and Medical Research Council (NHMRC, Australia). Male mice were used for all experiments. Wild-type (C57BL/10) and dystrophic *mdx* mice were sourced from the Animal Resources Centre (Canning Vale, Western Australia).

Muscle functional analysis. Mice were anaesthetized with sodium pentobarbitone (Nembutal) such that they were unresponsive to tactile stimuli. Contractile properties of diaphragm muscle strips were assessed *in vitro*.

Morphological analysis. Muscles were trimmed of tendons and adhering non-muscle tissue, mounted in embedding medium, frozen in liquid-nitrogen-cooled isopentane, and stored at −80 °C. Transverse muscle sections were cryosectioned from the mid-belly of each muscle. Muscle collagen content was assessed from Van Gieson's stained cross-sections that were quantified.

SERCA activity assay. Ca^{2+}-dependent SERCA activity was assessed in isolated enriched SR vesicles and whole-muscle homogenates. For whole-muscle homogenates, muscles were surgically excised from anaesthetized mice and stored at −80 °C for subsequent analyses. For enriched SR vesicles, mixed hindlimb muscles (quadriceps, gastrocnemius, extensor digitorum longus, soleus and plantaris) and diaphragm muscles were homogenized and subjected to sucrose gradient differential centrifugation using a Thermo Scientific Sorvall WX100 ultracentrifuge with a T-890 fixed-angle rotor. During the entire homogenization and SR vesicle isolation procedures, samples were immersed in ice to avoid temperature-dependent decreases in SERCA activity.

Skeletal preparation. To reveal skeletal architecture, mice (after death) were skinned, eviscerated and placed in a KOH solution (1.5% w/v), for 5 days. KOH solution was replaced and a small amount of alizarin red was added to stain calcium deposits; the preparation was left for a further 5 days.

Full Methods and any associated references are available in the online version of the paper at www.nature.com/nature.

Received 30 January; accepted 21 February 2012.
Published online 4 April 2012.

1. Emery, A. E. The muscular dystrophies. *Lancet* **359,** 687–695 (2002).
2. Ervasti, J. M. & Campbell, K. P. Membrane organization of the dystrophin–glycoprotein complex. *Cell* **66,** 1121–1131 (1991).
3. Koenig, M., Monaco, A. P. & Kunkel, L. M. The complete sequence of dystrophin predicts a rod-shaped cytoskeletal protein. *Cell* **53,** 219–228 (1988).
4. Blake, D. J., Weir, A., Newey, S. E. & Davies, K. E. Function and genetics of dystrophin and dystrophin-related proteins in muscle. *Physiol. Rev.* **82,** 291–329 (2002).
5. Straub, V., Rafael, J. A., Chamberlain, J. S. & Campbell, K. P. Animal models for muscular dystrophy show different patterns of sarcolemmal disruption. *J. Cell Biol.* **139,** 375–385 (1997).
6. Turner, P. R., Westwood, T., Regen, C. M. & Steinhardt, R. A. Increased protein degradation results from elevated free calcium levels found in muscle from *mdx* mice. *Nature* **335,** 735–738 (1988).
7. Grady, R. M. *et al.* Skeletal and cardiac myopathies in mice lacking utrophin and dystrophin: a model for Duchenne muscular dystrophy. *Cell* **90,** 729–738 (1997).
8. Deconinck, A. E. *et al.* Utrophin-dystrophin-deficient mice as a model for Duchenne muscular dystrophy. *Cell* **90,** 717–727 (1997).
9. Gervasio, O. L., Whitehead, N. P., Yeung, E. W., Phillips, W. D. & Allen, D. G. TRPC1 binds to caveolin-3 and is regulated by Src kinase—role in Duchenne muscular dystrophy. *J. Cell Sci.* **121,** 2246–2255 (2008).
10. Fong, P. Y., Turner, P. R., Denetclaw, W. F. & Steinhardt, R. A. Increased activity of calcium leak channels in myotubes of Duchenne human and *mdx* mouse origin. *Science* **250,** 673–676 (1990).
11. Bellinger, A. M. *et al.* Hypernitrosylated ryanodine receptor calcium release channels are leaky in dystrophic muscle. *Nature Med.* **15,** 325–330 (2009).
12. Nicolas-Metral, V., Raddatz, E., Kucera, P. & Ruegg, U. T. Mdx myotubes have normal excitability but show reduced contraction–relaxation dynamics. *J. Muscle Res. Cell Motil.* **22,** 69–75 (2001).

©2012 Macmillan Publishers Limited. All rights reserved

13. Tutdibi, O., Brinkmeier, H., Rudel, R. & Fohr, K. J. Increased calcium entry into dystrophin-deficient muscle fibres of MDX and ADR-MDX mice is reduced by ion channel blockers. *J. Physiol. (Lond.)* **515,** 859–868 (1999).
14. Goonasekera, S. A. *et al.* Mitigation of muscular dystrophy in mice by SERCA overexpression in skeletal muscle. *J. Clin. Invest.* **121,** 1044–1052 (2011).
15. Morine, K. J., Sleeper, M. M., Barton, E. R. & Sweeney, H. L. Overexpression of SERCA1a in the *mdx* diaphragm reduces susceptibility to contraction-induced damage. *Hum. Gene Ther.* **12,** 1735–1739 (2010).
16. Porter, J. D. *et al.* A chronic inflammatory response dominates the skeletal muscle molecular signature in dystrophin-deficient *mdx* mice. *Hum. Mol. Genet.* **11,** 263–272 (2002).
17. Acharyya, S. *et al.* Interplay of IKK/NF-κB signaling in macrophages and myofibres promotes muscle degeneration in Duchenne muscular dystrophy. *J. Clin. Invest.* **117,** 889–901 (2007).
18. Kolodziejczyk, S. M. *et al.* Activation of JNK1 contributes to dystrophic muscle pathogenesis. *Curr. Biol.* **11,** 1278–1282 (2001).
19. Monici, M. C., Aguennouz, M., Mazzeo, A., Messina, C. & Vita, G. Activation of nuclear factor-κB in inflammatory myopathies and Duchenne muscular dystrophy. *Neurology* **60,** 993–997 (2003).
20. Senf, S. M., Dodd, S. L., McClung, J. M. & Judge, A. R. Hsp70 overexpression inhibits NF-κB and Foxo3a transcriptional activities and prevents skeletal muscle atrophy. *FASEB J.* **22,** 3836–3845 (2008).
21. Park, H. S., Lee, J. S., Huh, S. H., Seo, J. S. & Choi, E. J. Hsp72 functions as a natural inhibitory protein of c-Jun N-terminal kinase. *EMBO J.* **20,** 446–456 (2001).
22. Chung, J. *et al.* HSP72 protects against obesity-induced insulin resistance. *Proc. Natl Acad. Sci. USA* **105,** 1739–1744 (2008).
23. Tupling, A. R. *et al.* HSP70 binds to the fast-twitch skeletal muscle sarco(endo)plasmic reticulum Ca^{2+}-ATPase (SERCA1a) and prevents thermal inactivation. *J. Biol. Chem.* **279,** 52382–52389 (2004).
24. Bornman, L., Polla, B. S., Lotz, B. P. & Gericke, G. S. Expression of heat-shock/stress proteins in Duchenne muscular dystrophy. *Muscle Nerve* **18,** 23–31 (1995).
25. Lou, J. S., Weiss, M. D. & Carter, G. T. Assessment and management of fatigue in neuromuscular disease. *Am. J. Hosp. Palliat. Care* **27,** 145–157 (2010).
26. Finsterer, J. Cardiopulmonary support in Duchenne muscular dystrophy. *Lung* **184,** 205–215 (2006).
27. Stedman, H. H. *et al.* The *mdx* mouse diaphragm reproduces the degenerative changes of Duchenne muscular dystrophy. *Nature* **352,** 536–539 (1991).
28. Briguet, A., Courdier-Fruh, I., Foster, M., Meier, T. & Magyar, J. P. Histological parameters for the quantitative assessment of muscular dystrophy in the *mdx*-mouse. *Neuromuscul. Disord.* **14,** 675–682 (2004).
29. Literati-Nagy, B. *et al.* Improvement of insulin sensitivity by a novel drug, BGP-15, in insulin-resistant patients: a proof of concept randomized double-blind clinical trial. *Horm. Metab. Res.* **41,** 374–380 (2009).
30. Morimoto, R. I. Cells in stress: transcriptional activation of heat shock genes. *Science* **259,** 1409–1410 (1993).

Supplementary Information is linked to the online version of the paper at www.nature.com/nature.

Acknowledgements We thank R. Koopman, J. G. Ryall and G. I. Lancaster for comments; J. Trieu, B. G. Gleeson, T. Naim and A. Chee for technical support; and C. Angelini and the Neuromuscular bank of tissues and DNA samples – Telethon Network of Genetic Biobanks for the provision of human muscle specimens. We thank N-Gene R&D Inc. USA for providing the BGP-15 compound. This study was supported in part by research grants from the National Health and Medical Research Council (NHMRC; project numbers 1009114 to G.S.L. and 472650 and 1004441 to M.A.F.), Association Française contre les Myopathies (France, to G.S.L.) and the Muscular Dystrophy Association (USA, to G.S.L.). M.A.F. is a Senior Principal Research Fellow of the NHMRC. A.P.R. was supported by a NHMRC Biomedical career Development Award. S.L. was supported by a postdoctoral fellowship from the Swiss National Science Foundation. S.M.G. was supported by a National Heart Foundation Postgraduate Scholarship (Australia). D.C.H. was supported by a National Heart Foundation Post-Doctoral Fellowship.

Author Contributions S.M.G., J.D.S., C.v.d.P., M.A.F. and G.S.L. conceived and designed the experiments. S.M.G., T.A.S., C.v.d.P., D.C.H. and J.E.C. performed the experiments. M.A.F. and K.E.D. facilitated experiments through the provision of mice and experimental compounds. A.P.R. and S.L. performed experiments on muscle samples from patients with DMD and from controls. S.M.G., D.C.H., M.A.F., C.v.d.P. and G.S.L. analysed the data. S.M.G. and G.S.L. wrote the manuscript. All authors checked for scientific content and contributed to the final drafting of the manuscript.

Author Information Reprints and permissions information is available at www.nature.com/reprints. The authors declare competing financial interests: details accompany the paper on www.nature.com/nature. Readers are welcome to comment on the online version of this article at www.nature.com/nature. Correspondence and requests for materials should be addressed to G.S.L. (gsl@unimelb.edu.au).

©2012 Macmillan Publishers Limited. All rights reserved

METHODS

Animals. Female *mdx* mice were crossed with male mice expressing a rat inducible Hsp72 transgene under the control of a β-actin promoter[31]. F_1 generation males were mated with female *mdx* mice to yield an equal proportion of $mdx^{TG(+)}$ and $mdx^{TG(-)}$ littermate controls. $WT^{TG(-)}$ and $WT^{TG(+)}$ mice were generated as described previously[22]. Genotyping was performed by PCR using primers described previously[32]. C57BL/10 and *mdx* mice used for heat therapy and BGP-15 treatment studies were obtained from the Animal Resources Centre (Canning Vale, Western Australia). Dystrophic *mdx* mice were treated from 4 weeks to 9 weeks of age (5 weeks) or from 4 weeks to 16 weeks of age (12 weeks) with BGP-15 (15 mg kg^{-1} per day, oral gavage; N-Gene R&D Inc.). BGP-15 is a pharmacological inducer of Hsp72, which has been shown to be safe and well tolerated in FDA-approved Phase II clinical trials for diabetes and insulin resistance[29,33]. For heat therapy, the mice were anaesthetized and the core body temperature was raised to about 40 °C with an infrared thermometer for 30 min every fourth day; body temperature was monitored from the external auditory meatus as described previously[34]. The *dko* mice were bred in the Biological Research Facility at the University of Melbourne[8]. The *dko* mice are utrophin-null on an *mdx* background and show a severe and progressive muscular dystrophy that more closely mimics the phenotypic characteristics of DMD[7,8]. The *dko* mice were treated with BGP-15 from 3–4 weeks to 10 weeks of age. For the survival study, *dko* mice were treated from 3–4 weeks until death or humane killing in accordance with the Animal Ethics Committee of The University of Melbourne (AEC). All experiments were approved by the AEC and conducted in accordance with the Australian code of practice for the care and use of animals for scientific purposes as stipulated by the National Health and Medical Research Council (Australia). Male mice were used for all experiments.

Muscle functional analyses. Mice were anaesthetized with sodium pentobarbitone (Nembutal; 60 mg kg^{-1} intraperitoneal; Sigma-Aldrich, New South Wales, Australia) such that they were unresponsive to tactile stimuli. Contractile properties of diaphragm muscle strips were assessed *in vitro* as described in detail previously[37]. In brief, strips of diaphragm muscle were bathed in oxygenated Krebs solution at 25 °C in a custom-made organ bath. Preparations were stimulated by supramaximal 0.2-ms square-wave pulses of 450 ms duration delivered by means of platinum plate electrodes flanking both sides of the muscle. Contractile properties of the TA muscle were assessed *in situ*[35]. In brief, TA muscles maintained at 37 °C were stimulated by supramaximal (14 V) 0.2-ms square-wave pulses of 350 ms duration delivered by means of two wire electrodes resting on the peroneal nerve. All muscles were adjusted to optimum muscle length (L_o), determined from maximum isometric twitch force (P_t). Maximum isometric tetanic force (P_o) was recorded from the plateau of the frequency–force relationship, and normalized to muscle cross-sectional area (specific force; sP_o), for comparisons between groups where appropriate[36–38]. The susceptibility of TA and diaphragm muscles to contraction-induced injury was determined from the protocols that we have described in detail previously[36–38]. Isolated muscles were maximally activated to produce isometric force and then stretched to perform an eccentric contraction (at a velocity of $2L_f s^{-1}$) at progressively increasing magnitudes of stretch. Maximum isometric force was determined before each eccentric contraction[37].

Morphological analysis. Muscles were trimmed of tendons and adhering non-muscle tissue, mounted in embedding medium, frozen in liquid-nitrogen-cooled isopentane, and stored at −80 °C. Transverse muscle sections (5 μm) were cryosectioned from the mid-belly of each muscle. Sections were stained with haematoxylin/eosin to reveal general muscle architecture. Cross-sectional area (CSA) and minimal Feret's diameter was assessed in about 500 fibres from each section of diaphragm muscle, with the use of Carl Zeiss software (Axiovision 4.6.3). The minimal Feret's diameter is the minimum distance between opposing parallel tangents of a muscle fibre[39], and the variance coefficient is a highly sensitive parameter used for detecting differences between dystrophic and otherwise healthy muscles[39]. Muscle collagen content was assessed from Van Gieson's stained cross-sections that were quantified with Axiovision 4.6.3 software.

Enriched SR isolation. Mixed hindlimb muscles (quadriceps, gastrocnemius, extensor digitorum longus, soleus and plantaris) and diaphragm muscles were diluted in ice-cold homogenization buffer (250 mM sucrose, 5 mM HEPES pH 7.0, 0.2% NaN_3). Protease inhibitor cocktail (P-8340; Sigma-Aldrich, Castle Hill, New South Wales, Australia) was added immediately before homogenization at 5 μl per 100 mg muscle wet weight. The muscles were minced on ice with surgical scissors and homogenized with a Polytron homogenizer (PT2100; Kinematica, Inc. Dispersing and Mixing Technology, New York) at a power setting of 21 for three 20-s bursts separated by 45-s breaks on ice. To obtain a purified and enriched SR membrane fraction, the homogenates were centrifuged at 5,500*g* for 10 min at 4 °C to remove insoluble material. The supernatants were harvested and centrifuged at 12,500*g* for 18 min at 4 °C. The pellet was discarded and the supernatant was centrifuged for a second time at 12,500*g* for 18 min at 4 °C. Supernatants were transferred to ultracentrifuge tubes, which were balanced and centrifuged at 50,000*g* (24,200 r.p.m. on a T-890 fixed-angle rotor; Thermo Scientific Sorvall WX100 ultracentrifuge) for 1 h at 4 °C. Supernatants were discarded and pellets were resuspended in 5 ml of homogenization buffer containing 600 mM KCl and incubated on ice for 30 min. Samples were centrifuged at 15,000*g* for 10 min at 4 °C to pellet and remove mitochondria. Supernatants were centrifuged again at 50,000*g* for 1 h at 4 °C. The final pellet (enriched SR membrane vesicles) was resuspended in homogenization buffer. Protein content was determined in triplicate[40].

SERCA activity assay. Ca^{2+}-dependent SERCA activity was assessed in isolated enriched SR vesicles and whole-muscle homogenates on the basis of the methods of Leberer and colleagues, as described previously[41]. For whole-muscle homogenates, muscles were surgically excised from anaesthetized mice and stored at −80 °C. Muscle samples (about 20–50 mg) were diluted in about 200 μl of ice-cold homogenization buffer. Protease inhibitor cocktail (P-8340) was added immediately before use at a concentration of 5 μl per 100 mg of muscle tissue. Muscles were homogenized with a hand-held glass homogenizer, and then centrifuged for 10 min at 5,500*g* at 4 °C. Supernatant protein concentration was determined in triplicate[40]. Protein concentration was adjusted to 10 mg ml^{-1}, when possible, with homogenization buffer. SERCA activity in whole-muscle homogenates was determined in reaction buffer (200 mM KCl, 20 mM HEPES, pH 7.0, 15 mM $MgCl_2$, 10 mM NaN_3, 10 mM phosphoenolpyruvate, 5 mM ATP, 1 mM EGTA). SERCA activity in enriched SR vesicles was determined in reaction buffer (100 mM KCl, 20 mM HEPES, 10 mM $MgCl_2$, 10 mM NaN_3, 10 mM phosphoenolpyruvate, 5 mM ATP, and 1 mM EGTA). The pH of both reaction buffers was adjusted to 7.0 at 37 °C. Immediately before starting the reaction, 18 U ml^{-1} PK, 18 U ml^{-1} lactate dehydrogenase (LDH), 5 μl NADH (100 mM), 1 μM calcimycin A-23187 (Sigma-Aldrich) and about 10 μl of whole-muscle homogenate or about 3 μl of enriched SR vesicles were added to 1 ml of reaction buffer in a plastic cuvette. Cuvettes were loaded into a spectrophotometer and A_{340} was measured at 37 °C (Multiscan Spectrum; Thermo Electron, Waltham, Massachusetts). Maximal (V_{max}) and Ca^{2+}-dependent SERCA activities were determined by progressively adding Ca^{2+} until a plateau or maximal activity was reached. The specific SERCA inhibitor 2′,5′-di(tert-butyl)-1,4-benzohydroquinone (TBQ) was added to a final concentration of 40 μM to determine basal activity. SERCA enzyme kinetic parameters, determined from a regression analysis, were the Ca^{2+} concentration required to elicit 50% maximal SERCA activity ($[Ca^{2+}]_{50}$) and the Hill coefficient, which is a measure of the cooperativity of Ca^{2+} binding of the SERCA enzyme. SERCA activity was graphed against added Ca^{2+} concentration. Non-regression analysis was performed using the following variable-slope sigmoidal dose–response relationship, using Graphpad Prism v. 3.02 (GraphPad Software Inc., San Diego):

$$Y = Y_{bottom} + Y_{top} - \frac{Y_{bottom}}{1 + 10^{\log[Ca]_{50} - X} n_H}$$

Peroxynitrite-mediated SERCA inhibition assay. SERCA activity in enriched SR vesicles after incubation in various concentrations of peroxynitrite ($[ONOO^-]$) was measured. $[ONOO^-]$ was measured spectrophotometrically ($\varepsilon = 1{,}670\ M\ cm^{-1}$ at 302 nm, about 68 mM in stock). Enriched SR vesicle samples were added to reaction buffer (as described previously) in the presence of $ONOO^-$ (0, 10, 50, 100, 250, 500 or 1,000 μM) and incubated for 5 min at 37 °C in a plastic cuvette. $ONOO^-$ and byproducts were quenched by the addition of 1 mM dithiothreitol (to prevent the inactivation of PK and LDH subsequently added); 18 U ml^{-1} PK, 18 U ml^{-1} LDH and 5 μl of NADH (100 mM) were then added. Cuvettes were loaded into a spectrophotometer, and A_{340} was measured at 37 °C. Maximal SERCA activity was determined by adding Ca^{2+} until a plateau or maximal activity was reached. Once maximal activity had been determined, the specific SERCA inhibitor TBQ was added to a final concentration of 40 μM to determine basal activity. Maximal SERCA activity in each sample was assessed independently at various $ONOO^-$ concentrations (10, 50, 100, 250, 500 or 1,000 μM) and expressed as a percentage of the maximal SERCA activity in the absence of $ONOO^-$.

Human DMD samples. Human muscle specimens were sourced from the Telethon Network of Genetic Biobanks, Italy. Biopsies were taken from the vastus lateralis muscle of patients with DMD (aged 1–9 years) or healthy controls (aged 18–25 years) using either a Bergström or open biopsy technique. All biopsies were frozen immediately in liquid nitrogen and stored at −80 °C until analysis. Muscle samples were homogenized in RIPA buffer (Millipore, Billerica, Massachusetts) and rotated for 1 h at 4 °C, followed by centrifugation for 15 min at 4 °C. The supernatant was collected and protein concentration was determined by means of the bicinchoninic acid protein assay (Pierce Biotechnology). Electrophoresis was performed by 10% SDS–PAGE in a buffer containing 12 mM Tris-HCl pH 8.8,

©2012 Macmillan Publishers Limited. All rights reserved

200 mM glycine and 0.1% SDS. Protein transfer was performed in a buffer containing 12 mM Tris-HCl pH 8.3, 200 mM glycine and 10% methanol with the use of poly(vinylidene difluoride) membranes. The membranes were blocked with 5% BSA in PBS, after which they were incubated overnight at 4 °C with the primary antibody against Hsp70 (SPA-812; Stressgen) diluted 1:1000 in PBS. After being washed, the membranes were incubated for 1 h with a goat anti-rabbit IgG antibody labelled with an infrared-fluorescent 800-nm dye (Alexa Fluor 800; Invitrogen) diluted 1:5,000 in PBS containing 50% Odyssey blocking buffer (LI-COR Biosciences) and 0.01% SDS. After being washed, the proteins were exposed on an Odyssey Infrared Imaging System (LI-COR Biosciences) and individual protein band optical densities were determined with ImageJ Software (National Institutes of Health). The blots were normalized against glyceraldehyde-3-phosphate dehydrogenase (GAPDH) protein (G8795; Sigma-Aldrich, Sydney, Australia).

Evans blue dye uptake. To quantify muscle damage and areas of focal necrosis, EBD (1% w/v) was injected intraperitoneally (10 μl per gram body mass). Muscles were frozen 20 h after the EBD injection. Sections 10 μm thick were cut on a cryostat, and EBD was detected as red autofluorescence with the use of a fluorescence microscope.

Wire hang test. A wire hang test was employed to assess whole-body muscle strength and endurance. Mice were placed on a wire mesh grid, which they gripped; the grid was then inverted. Latency-to-fall onto a padded surface was recorded in three successive trials, with the average of the best two trials used for analyses.

Single muscle fibre analysis. Mice were anaesthetized with sodium pentobarbitone (Nembutal) such that they were unresponsive to tactile stimuli, and the extensor digitorum longus and/or soleus muscle was surgically excised for single fibre analysis. The muscle was blotted on filter paper and placed in a Petri dish containing paraffin oil at room temperature (23 ± 2 °C). Muscles were pinned at resting length to the base of a dish. Single muscle fibres were isolated from as close to the surface of the muscle as possible, and fine forceps were used to peel the sarcolemma away from the contractile apparatus under a dissecting microscope. The mechanically skinned fibre was then attached to one end of a piezoresistive force transducer (AE801 SensoNor; Horten) using braided silk (size 10, 0.2 mm; Deknatel), and the other end of the fibre was clamped between a pair of forceps fixed to a micromanipulator. All experiments were conducted at room temperature. All solutions had pH of 7.10 ± 0.01, and the free Mg^{2+} concentration ([Mg^{2+}]) was 1 mM, unless specified otherwise. Free [Ca^{2+}] at 0.1 μM or more was verified with a Ca^{2+}-sensitive electrode (Orion Research).

Caffeine-induced force responses and SR Ca^{2+} accumulation. Initially, mechanically skinned muscle fibres were equilibrated for 30 s in a wash solution followed by thorough depletion of SR Ca^{2+} stores, achieved by transferring the fibre preparation into a release solution containing 30 mM caffeine and 0.02 mM free Mg^{2+}. The presence of 0.5 mM EGTA in the release solution ensured that the level of Ca^{2+} during caffeine-induced release did not maximally activate the contractile apparatus, which is necessary to allow quantitative evaluation of the amount of Ca^{2+} released. Ca^{2+} release from the SR was estimated from the relative areas under the caffeine-induced force response. The fibre was left in the release solution for 2 min to ensure complete SR Ca^{2+} depletion, before being washed for 30 s. Thereafter, the SR was reloaded with Ca^{2+} in load solution (0.2 μM Ca^{2+} (pCa 6.7), where $pCa = -\log_{10}[Ca^{2+}]$) for increasing durations (10, 20, 30 and 60 s), before being equilibrated for 30 s in wash solution; subsequently, SR Ca^{2+} was released in release solution. Data were fitted with a standard exponential association equation to give the rate at which the SR accumulated Ca^{2+} (in s^{-1}) but not the amount of SR Ca^{2+} accumulated. SR accumulation is an indirect measure of SERCA activity[42].

SR Ca^{2+} leak. The percentage of Ca^{2+} lost from the SR as a result of the passive leak was also assessed. The fibre was loaded for 20 s in loading solution. The fibre preparation was then placed in wash solution for 30 s followed by SR Ca^{2+} content released in release solution (Ca^{2+} leak in 30 s). The fibre preparation was placed in wash solution before reloading for 20 s in load solution and transferred to wash solution for 90 s; the remaining SR Ca^{2+} was released in release solution (Ca^{2+} leak in 90 s). The 30-s Ca^{2+} leak was then repeated, and the area (corrected for proportionality between area and SR Ca^{2+} content) under the test run was divided by the average of the areas under the caffeine-induced force responses in the controls before and after the test run. This gave an estimate of the fraction of SR Ca^{2+} leaked over a 60-s leak period.

Relative SR Ca^{2+} sensitivity. To determine the effect of Hsp72 overexpression on the ryanodine receptor (RyR), a caffeine dose–response curve was determined from the forces produced by the contractile apparatus after SR Ca^{2+} release induced by low caffeine concentrations. Each fibre was prepared by completely depleting the SR of Ca^{2+} with 30 mM caffeine followed by a 30-s SR Ca^{2+} reloading duration. The peak force of caffeine-induced contraction was determined in a series of potassium hexamethylene-diamine tetraacetic acid solutions containing 2, 3, 5 and 7 mM caffeine and 50 μM EGTA, with complete SR Ca^{2+} depletion and 30-s reloading duration of the SR with Ca^{2+} between each caffeine contraction. The peaks of the caffeine-induced contractions were then normalized as a percentage of maximum Ca^{2+}-activated force to estimate the sensitivity of the RyR to caffeine. This determined whether overexpression of Hsp72 directly affected the function of the RyR.

Properties of the contractile apparatus. After SR properties were investigated, the single muscle fibres were equilibrated in a relaxing solution (pCa > 9) for 2 min. Fibres were placed in a maximum Ca^{2+}-activating solution (pCa ≈ 4.5) until force reached the maximal value (maximum Ca^{2+}-activated force) and then placed back in the relaxing solution for a further 2 min. Force responses were generated by exposing the fibre to activating solutions of progressively lower pCa (higher [Ca^{2+}]) in a stepwise fashion. The force response generated at each pCa was expressed as a percentage of the interpolated values for maximum Ca^{2+}-activated force. Data points were fitted with a Hill equation producing two parameters: the pCa_{50} (the pCa producing half-maximum force) and n_H (the Hill coefficient, indicative of the steepness of the force–pCa relationship).

Western blotting. After the determination of SERCA activity in whole-muscle homogenates and enriched SR vesicles, electrophoresis was performed on the same samples for the quantification of protein expression. Equal amounts of protein were resolved in SDS buffer, heated for 5 min at 95 °C and separated on SDS-polyacrylamide gels. Separated proteins were transferred to poly(vinylidene difluoride) membranes (0.45-μm Immobilon-P; Millipore). Membranes were blocked with 5% non-fat milk powder (or BSA) in Tris-buffered saline containing Tween 20 for 1 h and incubated overnight at 4 °C with appropriate antibody dilutions. Antibodies against SERCA 1 (Affinity Bioreagents), SERCA 2a (Affinity Bioreagents), Hsp72 (Stressgen), α-tubulin (ECM-Biosciences) and GAPDH (Sigma) were used. Membranes were digitized with a chemiluminescent detection and imaging system (ChemiDoc XRS; Bio-Rad Laboratories, Hercules, California, USA) and band densities were quantified with Quantity One analysis software (version 4.6.1; Bio-Rad Laboratories).

Real-time PCR. Real-time PCR was performed as described previously[43]. Each sample was run in triplicate. The mean reading of each triplicate was converted to an absolute content by using a DNA standard curve, based on a serial dilution of DNA standard (100–10,000 ng ml^{-1}; Molecular Probes) run together with the samples on each plate. Gene expression was quantified by normalizing the logarithmic cycle threshold (C_t) value (2_{C_t}) to the cDNA content of each sample to obtain the expression 2_{C_t}/cDNA content (ng ml^{-1}). In Supplementary Fig. 5b, mRNA for SERCA 1 and SERCA 2a was normalized to the eukaryotic 18S housekeeping gene.

Creatine kinase analysis. Serum CK activity was analysed as an overall measure of whole-body muscle breakdown. Blood was collected from the tail vein and centrifuged for 10 min at 10,000*g* and 4 °C to isolate the serum fraction. Serum CK activity was then determined with a commercially available creatine kinase assay kit (ECPK-100) in accordance with the manufacturer's instructions (BioAssay Systems).

Skeletal preparation. Skeletal architecture was revealed as described previously[44]. After death, the mice were skinned, eviscerated and placed in a KOH solution (1.5% w/v), for 5 days. KOH solution was replaced and a small amount of alizarin red was added to stain calcium deposits; the preparation was left for a further 5 days to produce the specimens shown in Fig. 4a.

Statistical analysis. All values are presented as means ± s.e.m. Unpaired Student's *t*-tests were used to compare between two groups. When comparisons were being made between more than two groups, a one-way analysis of variance was used with Newman–Keuls post-hoc multiple comparison test.

31. Marber, M. S. *et al.* Overexpression of the rat inducible 70-kD heat stress protein in a transgenic mouse increases the resistance of the heart to ischemic injury. *J. Clin. Invest.* **95,** 1446–1456 (1995).
32. Taleb, M. *et al.* Hsp70 inhibits aminoglycoside-induced hair cell death and is necessary for the protective effect of heat shock. *J. Assoc. Res. Otolaryngol.* **9,** 277–289 (2008).
33. Literati-Nagy, B. *et al.* Beneficial effect of the insulin sensitizer (HSP inducer) BGP-15 on olanzapine-induced metabolic disorders. *Brain Res. Bull.* **20,** 340–344 (2010).
34. Saegusa, Y. & Tabata, H. Usefulness of infrared thermometry in determining body temperature in mice. *J. Vet. Med. Sci.* **65,** 1365–1367 (2003).
35. Gregorevic, P., Plant, D. R., Leeding, K. S., Bach, L. A. & Lynch, G. S. Improved contractile function of the *mdx* dystrophic mouse diaphragm muscle after insulin-like growth factor-I administration. *Am. J. Pathol.* **161,** 2263–2272 (2002).
36. Schertzer, J. D., Ryall, J. G. & Lynch, G. S. Systemic administration of IGF-I enhances oxidative status and reduces contraction-induced injury in skeletal muscles of *mdx* dystrophic mice. *Am. J. Physiol.* **291,** 499–505 (2006).
37. Schertzer, J. D., Gehrig, S. M., Ryall, J. G. & Lynch, G. S. Modulation of insulin-like growth factor (IGF)-I and IGF-binding protein interactions enhances skeletal

©2012 Macmillan Publishers Limited. All rights reserved

muscle regeneration and ameliorates the dystrophic pathology in *mdx* mice. *Am. J. Pathol.* **171,** 1180–1188 (2007).
38. Gehrig, S. M., Koopman, R., Naim, T., Tjoakarfa, C. & Lynch, G. S. Making fast-twitch dystrophic muscles bigger protects them from contraction injury and attenuates the dystrophic pathology. *Am. J. Pathol.* **176,** 29–33 (2010).
39. Briguet, A., Courdier-Fruh, I., Foster, M., Meier, T. & Magyar, J. P. Histological parameters for the quantitative assessment of muscular dystrophy in the *mdx*-mouse. *Neuromuscul. Disord.* **14,** 675–682 (2004).
40. Bradford, M. M. A rapid and sensitive method for the quantitation of microgram quantities of protein utilizing the principle of protein-dye binding. *Anal. Biochem.* **72,** 248–254 (1976).
41. Schertzer, J. D. *et al.* β_2-Agonist administration increases sarcoplasmic reticulum Ca^{2+}-ATPase activity in aged rat skeletal muscle. *Am. J. Physiol.* **288,** 526–533 (2005).
42. Plant, D. R. & Lynch, G. S. Depolarization-induced contraction and SR function in mechanically skinned muscle fibres from dystrophic *mdx* mice. *Am. J. Physiol.* **285,** C522–C528 (2003).
43. Murphy, K. T. *et al.* Antibody-directed myostatin inhibition in 21-mo-old mice reveals novel roles for myostatin signaling in skeletal muscle structure and function. *FASEB J.* **24,** 4433–4442 (2010).
44. Green, M. C. A rapid method for clearing and staining specimens for the demonstration of bone. *Ohio J. Sci.* **52,** 31–33 (1952).

©2012 Macmillan Publishers Limited. All rights reserved